Polyhedron 67 (2014) 171–180

Contents lists available at ScienceDirect

Polyhedron

journal homepage: www.elsevier.com/locate/poly

Diiron(III) complexes of tridentate 3N ligands as functional models for methane monooxygenases: Effect of the capping ligand on hydroxylation of alkanes

Muniyandi Sankaralingam [a], Mallayan Palaniandavar [b,*]

[a] School of Chemistry, Bharathidasan University, Tiruchirappalli 620024, Tamil Nadu, India
[b] Department of Chemistry, Central University of Tamil Nadu, Thiruvarur 610004, Tamil Nadu, India

ARTICLE INFO

Article history:
Received 6 July 2013
Accepted 15 August 2013
Available online 12 September 2013

Keywords:
Diiron(III) complexes
Tridentate 3N ligands
Alkane hydroxylation
Iron-oxo intermediate

ABSTRACT

A series of non-heme (μ-oxo)bis(μ-benzoato)-bridged diiron(III) complexes of the type $[Fe_2(O)(OBz)_2(L)_2]^{2+}$ (**1**–**6**), where OBz = benzoate, L = bis(pyridin-2-ylmethyl)amine (L1), *N*-((6-methylpyridin-2-yl-)methyl)(pyridin-2-yl)methanamine (L2), *N*,*N*-dimethyl-*N*′-(pyrid-2-ylmethyl)ethylenediamine (L3), (1-methyl-1*H*-imidazol-2-yl)-*N*-(pyridin-2-ylmethyl)-methanamine (L4), (1*H*-benzo[o]imidazol-2-yl)-*N*-(pyridin-2-ylmethyl)methanamine (L5) and bis((1*H*-benzo[o]imidazol-2-yl)methyl)amine (L6), have been isolated and characterized by means of elemental analysis, spectral and electrochemical methods. They have been studied as catalysts for selective hydroxylation of alkanes using *m*-choloroperbenzoic acid (*m*-CPBA) as the oxidant. In acetonitrile/dichloromethane mixed solvent all the complexes display a d–d band characteristic of a triply bridged diiron(III) core, revealing that they retain their identity in solution. Upon replacing a donor atom on the capping ligand by a stronger donor, the $E_{1/2}$ value of the one-electron $Fe^{III}Fe^{III} \rightarrow Fe^{III}Fe^{II}$ reduction becomes more negative. All the complexes function as efficient catalysts for hydroxylation of cyclohexane, with 390–410 total turnover numbers and good alcohol selectivity (A/K, 9.3–12.8). Adamantane is selectively oxidized (3°/2°, 15.7–28.1) to 1-adamantanol and 2-adamantanol, along with a small amount of 2-adamantanone (Total TON, 336–437), and interestingly the 3N capping ligands with the pyridyl donor around the diiron(III) center lead to high 3°/2° bond selectivity.

1. Introduction

The selective hydroxylation of hydrocarbons under mild conditions is an exciting and challenging scientific goal in bioinorganic and synthetic organic chemistry [1] because conventional hydroxylation processes usually require high pressures and high temperatures, while enzymes catalyze these reactions very efficiently with high selectivity under mild reaction conditions. This indicates that enzymatic reactions follow methodologies different from those of traditional synthetic processes. In nature, iron containing enzymes, like methane monooxygenases, bleomycin and cytochrome P450, play a vital role in catalyzing many biologically necessary organic transformations. Particularly, soluble methane monooxygenases (sMMO), which catalyze the oxidation of methane to methanol using dioxygen, are widely investigated metalloenzymes [2–11]. Thus the active site of the oxidized form of sMMO possesses a diiron(III) center consisting of only one carboxylate and two hydroxo bridges (sMMOox, Scheme 1). On the other hand, the reduced form of sMMO possesses a diiron(II) center containing four glutamate and two histidine residues, and the iron atoms are bridged by two carboxylate ligands from glutamate residues (sMMOred, Scheme 1) [12–14]. It is interesting that a number of non-heme diiron proteins, such as hemerythrin (Hr) [15] and ribonucleotide reductases (RNR) [16–18], also contain at least two carboxylate bridges in the active site of their reduced forms, but they exhibit differences in their functional aspects. Interestingly, the bridging units also play a vital role in dictating the functions of the enzyme. So, the isolation and study of synthetic models containing the structural motif $[Fe_2(O)(O_2CR)_2]^{2+}$ have received considerable interest amongst chemical and biochemical communities [19–23]. Also, a wide variety of coordination environments and bridging modes around the iron center in non-heme enzymes generate distinct oxidizing intermediates, which are supposed to result in their native catalytic transformations [11,24–29]. Encouraged by these enzymes, efforts have been made during the last two decades to develop synthetic models for sMMO in order to study the mechanism of O_2 activation involved in the oxygenation of alkanes [30,31]. The study of synthetic diiron complexes with different carboxylate motifs has mainly served as benchmarks for

* Corresponding author. Tel.: +91 9489079402; fax: +91 4366225312.
E-mail address: palanim51@yahoo.com (M. Palaniandavar).

0277-5387/$ - see front matter © 2013 Elsevier Ltd. All rights reserved.
http://dx.doi.org/10.1016/j.poly.2013.08.067

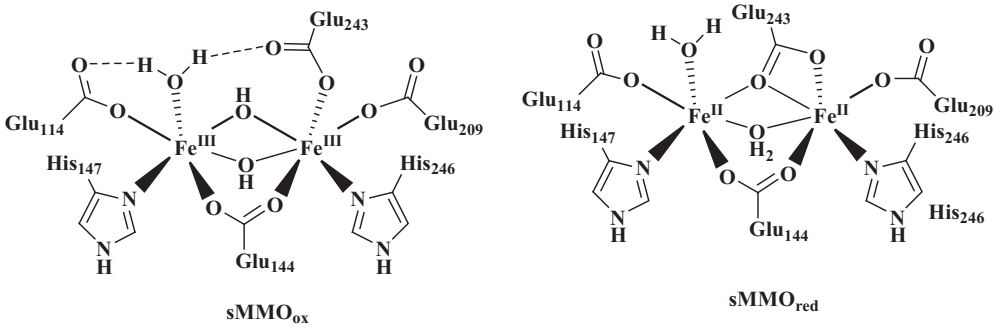

Scheme 1. Active site structures of soluble methane monooxygenases.

illustrating the oxidizing intermediates and catalytic pathway of the enzymes, and efforts to make use of them as functional mimics are fewer.

Several synthetic models containing the structural motif $[Fe_2(O)(O_2CR)_2(L)_2]^{2+}$, where L is a tridentate 3N ligand, have been isolated and studied as structural and functional models for metHr and sMMO [32–35]. Christou et al. [36,37] synthesized triply-bridged diiron(III) complexes derived from bipyridine for alkane hydroxylation, using *tert*-butylhydroperoxide (*t*-BuOOH) as the oxygen source, while Kitajima et al. [38] have isolated triply-bridged diiron(III) complexes resulting from the trispyrozolylborate ligand for alkane hydroxylation using molecular oxygen (in the presence of an electron source), but low selectivity and poor yields were observed for these reactions.

Later, Kodera et al. [39–41] found that the complex $[Fe_2(O)(O_2CCH_3)_2(hexpy)](ClO_4)_2$, where hexpy is 1,2-bis [2-(bis(pyrid-2-ylmethyl))-6-pyridyl]ethane, exhibits a high activity with a remarkable alcohol/ketone ratio (A/K, 2.4) for the hydroxylation of cyclohexane and tertiary/secondary carbon ratio (3°/2°, 4.2) for monooxygenation of adamantane using *m*-chloroperbenzoic acid (*m*-CPBA). Recently, Itoh et al. [42] isolated the triply-bridged diiron(III) complex $[Fe_2(O)(O_2CCH_3)_2(L)](ClO_4)_2$, where L is the dinucleating carboxylate ligand 1,2-bis(*N*-benzyl-2-aminomethyl-6-pyridyl)ethane-*N*′,*N*′-diacetic acid, and observed higher selectivity for the hydroxylation of cyclohexane (A/K, 10.0) and monooxygenation of adamantane (3°/2°, 13.6) using hydrogen peroxide as the oxygen source. However, the reasons for the high selectivity, efficiency and the mode of action of these complexes in alkane hydroxylation remain unclear. Also, many oxo-bridged diiron(III) complexes of tetradentate ligands have been isolated [43–46,37,47–49] as synthetic models for diiron(III) biosites, but the catalytic efficiency and selectivity of these systems are lower than those of the enzymes.

All of the above observations prompted us to isolate diiron(III) complexes of tridentate (3N) ligands with various carboxylate bridging ligands and to study their use as functional models for alkane hydroxylation reactions catalyzed by sMMO. Very recently, we have reported [50] the triply-bridged diiron(III) complexes $[Fe_2O(^{i}Bu\text{-}bpa/Bz\text{-}bpa)_2(RCOO)_2]^{2+}$, where ^{i}Bu-bpa = *N*,*N*-bis (pyrid-2-ylmethyl)-*iso*-butylamine, Bz-bpa = *N*,*N*-bis(pyrid-2-ylmethyl)benzylamine, R = $-CH_3$ and $-C_6H_5$, which act as efficient catalysts (A/K, 10.2-13.8) towards alkane hydroxylation. This encouraged us to isolate very recently [51] a few more (μ-oxo)-bis(μ-carboxylato)diiron(III) complexes, $[Fe_2(O)(OOCR)_2(L)_2](ClO_4)_2$ where L = *N*,*N*-dimethyl-*N*′-(pyrid-2-ylmethyl)-ethylenediamine and R = $HCOO^-$, CH_3COO^-, $(CH_3)_3C\text{-}COO^-$, $PhCOO^-$, $(Ph)_2CHCOO^-$ and $(Ph)_3CCOO^-$, which exhibit high activity with a notable alcohol/ketone ratio (A/K, 6.0-10.1) for the hydroxylation of cyclohexane and tertiary/secondary carbon ratio (3°/2°, 12.9–17.1) for monooxygenation of adamantane using *m*-chloroperbenzoic acid (*m*-CPBA), and interestingly, the activity depends upon the bridging carboxylate group. Encouraged by the above reactions, we have now isolated a few more (μ-oxo)bis(μ-benzoato)diiron(III) complexes, $[Fe_2(O)(OBz)_2(L)_2](ClO_4)_2$ (**1**–**6**) where L is a tridentate 3N ligand, namely bis(pyridin-2-ylmethyl)-amine (L1), *N*-((6-methylpyridin-2-yl-)methyl)(pyridin-2-yl)methanamine (L2), (1-methyl-1*H*-imidazol-2-yl)-*N*-(pyridin-2-ylmethyl)-methanamine (L3), (1*H*-benzo[o]imidazol-2-yl)-*N*-(pyridin-2-ylmethyl)methanamine (L4), *N*,*N*-dimethyl-*N*′-(pyrid-2-ylmethyl)-ethylenediamine (L5) and bis((1*H*-benzo[o]imidazol-2-yl)methyl)amine (L6) (Scheme 2), as new synthetic analogues for sMMO and studied the steric and electronic effects of the 3N ligands on the highly selective hydroxylation of alkanes.

The single-crystal X-ray structure of **5** (Fig. 1) has been reported [51] by our laboratory and that of **6** has been reported earlier [52]. They show that each iron atom in the complexes is coordinated to one oxygen atom of the μ-oxo bridge and two oxygen atoms of both μ-carboxylato bridges, in addition to three nitrogen atoms of the 3N ligand. We have observed that all six complexes show efficient hydroxylation of cyclohexane (290–410 TON) and adamantane with approximately 335–440 turnover numbers and good selectivity (A/K ratio, 9.3–12.8; 3°/2°, 15.7–28.1), as tuned, interestingly, by varying one or both terminal nitrogen atoms of the capping ligand from the weakly coordinating $-NMe_2$ donor to the strongly coordinating pyridyl, imidazolyl and benzimidazolyl nitrogen donors.

2. Experimental

2.1. Materials

Pyridine-2-carboxaldehyde, 2-aminomethylpyridine, *N*,*N*-dimethylethylenediamine, 6-methylpyridine-2-carboxaldehyde, *N*-methylimidazole-2-carboxaldehyde, iminodiaceticacid iron(III) perchlorate hydrate, adamantane, *m*-chloroperbenzoic acid, sodium borohydride, tetra-*N*-butylammonium bromide (Aldrich), *o*-phenylenediamine, triethylamine, benzoic acid, glacial acetic acid, hydrochloric acid (Merck, India), cyclohexane (Ranbaxy) and ethanol (Hayman Limited, England) were used as received. Dichloromethane, diethylether, tetrahydrofu-

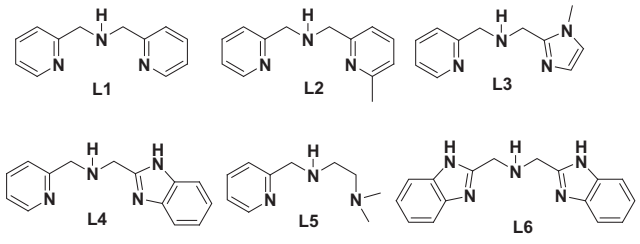

Scheme 2. Tridentate 3N ligands used in the study.

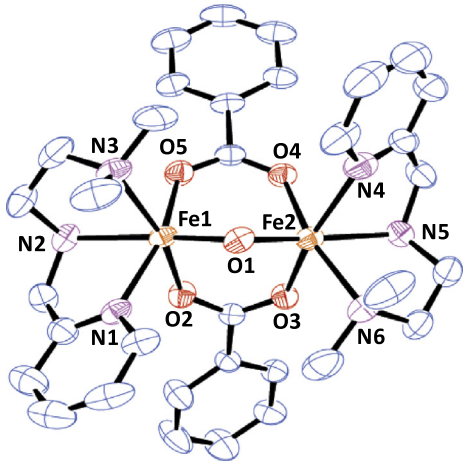

Fig. 1. ORTEP view of $[Fe_2O(L5)_2(OBz)_2]^{2+}$ **5** taken from [51] (40% probability factor for the thermal ellipsoids). Hydrogen atoms have been omitted for clarity.

ran, acetonitrile (Merck, India) and methanol (Sisco Research Laboratory, Mumbai) were distilled before use. The supporting electrolyte tetra-*N*-butylammonium perchlorate (TBAP) was prepared in water and recrystallized twice from aqueous ethanol.

2.2. Synthesis of the ligands

The ligands L1-L5 were prepared by using the procedures reported already [53–58]. The ligand L6 was prepared by the Phillips condensation reaction [59].

2.2.1. Bis(pyridin-2-ylmethyl)amine (L1) [53,54]

Pyridine-2-carboxaldehyde (1.07 g, 10 mmol) in methanol (20 mL) was added dropwise to aminomethylpyridine (1.08 g, 10 mmol) in methanol (20 mL). The mixture was stirred overnight and then $NaBH_4$ (0.57 g, 15 mmol) was added. The solution was stirred for another day and then rotary evaporated to dryness. The resulting solid was dissolved in water and then extracted with dichloromethane. The organic layer was dried with anhydrous sodium sulfate and then rotary evaporated to get the ligand as an oil. Yield: 1.72 g (86.4%); ^{1}H NMR (400 MHz, $CDCl_3$) δ (ppm): 8.48–7.29 (m, 8H), 4.12 (s, 4H). EI-MS *m*/*z*: 199 $C_{12}H_{13}N_3^+$.

2.2.2. N-((6-methylpyridin-2-yl-)methyl)(pyridin-2-yl)methanamine (L2)

The ligand L2 was synthesized using a modified procedure [53,54]. The aldehyde 6-methylpyridine-2-carboxaldehyde (1.23 g, 10 mmol) was used to obtain the L2 as a yellow oil, which was used for complex preparation without further purification. Yield: 1.48 g (69.4%); ^{1}H NMR (400 MHz, $CDCl_3$) δ (ppm): 8.48–7.29 (m, 7H), 4.12 (s, 4H), 2.61 (s, 3H). EI-MS *m*/*z*: 213 $C_{13}H_{15}N_3^+$.

2.2.3. (1-Methyl-1H-imidazol-2-ylmethyl)pyridin-2-ylmethylamine (L3)

The ligand L3 was synthesized using the same procedure [53–56] as followed for preparing L1. The aldehyde *N*-methyl-2-imidazolecarboxaldehyde (1.124 g, 10 mmol) was used to obtain L3 as a yellow oil, which was used for complex preparation without further purification. Yield: 1.27 g (62.9%); ^{1}H NMR (400 MHz, $CDCl_3$) δ (ppm): 8.44-7.26 (m, 4H), 6.72 (s, 1H), 6.62 (s, 1H), 4.14 (s, 2H), 3.81 (s, 2H), 3.63 (s, 3H). EI-MS *m*/*z*: 202 $C_{11}H_{14}N_4^+$.

2.2.4. (1H-benzo[o]imidazol-2-yl)-N-(pyridin-2-ylmethyl)-methanamine (L4)

The linear tridentate ligand L4 was synthesized by neutralizing 2-(aminomethyl)benzimidazole dihydrochloride [57,58] with K_2CO_3 and then condensing it with the corresponding pyridine-2-carboxaldehyde to form a Schiff base, followed by the reduction of the latter with sodium borohydride [53,54]. Yield: 1.32 g (55.4%); ^{1}H NMR (400 MHz, $CDCl_3$) δ (ppm): 8.52-7.32 (m, 8H), 4.04 (s, 2H), 3.82 (s, 2H). EI-MS *m*/*z*: 238 $C_{14}H_{14}N_4^+$.

2.2.5. N,N-dimethyl-N′-(pyrid-2-ylmethyl)ethylenediamine (L5)

The ligand L5 was synthesized using the same procedure [53,54] as followed for L1. The amine *N*,*N*-dimethylethylenediamine (0.927 g, 10 mmol) was used to obtain L5 as a yellow oil, which was used for complex preparation without further purification. Yield: 1.12 g (82%). ^{1}H NMR (400 MHz, $CDCl_3$) δ (ppm): 2.17 (s, 6H), 2.41 (t, 2H), 2.62 (t, 2H), 3.92 (s, 2H), 7.14 (t, H), 7.53 (d, H), 7.64 (t, H), 8.56 (d, H). EI-MS *m*/*z*: 179.14 $C_{10}H_{17}N_3^{\cdot+}$.

2.3. Isolation of the diiron(III) complexes

The general procedure involves the addition of carboxylic acids (2.0 mmol), previously neutralized with 2.0 mmol of triethylamine, to a mixture of $Fe(ClO_4)_3{\cdot}6H_2O$ (0.924 g, 2.0 mmol) in methanol (5 mL) containing H_2O (0.1 mL) and then stirring for 30 min at room temperature. To this, a methanol (8 mL) solution of the ligand (2.0 mmol) was added and the resulting dark red solution turned reddish brown or green upon stirring for an hour. Reddish brown or green precipitate or microcrystals of the diiron(III) complexes were formed within 24 h upon standing. The precipitate was collected by suction filtration, washed with small quantities of cold methanol and then dried *in vacuo*.

2.3.1. $[Fe_2(O)(OBz)_2(L1)_2](ClO_4)_2$ (**1**)

Complex **1** was prepared using the above general procedure using L1 (0.199 g, 1.0 mmol). Yield: 0.76 g (79%). ESI-MS, *m*/*z*: 866.87 $[(M-2H-ClO_4)^+]$, 744.87 $[(M-2H-BzO-ClO_4)^+]$, 383.93 $[(M-2H-2ClO_4)^{2+}]$. *Anal.* Calc. for $C_{38}H_{38}Fe_2N_6O_{13}Cl_2$: C, 47.08; H, 3.95; N, 8.67. Found: C, 47.12; H, 3.91 N, 8.62%.

2.3.2. $[Fe_2(O)(OBz)_2(L2)_2](ClO_4)_2$ (**2**)

Complex **2** was prepared using the above general procedure using L2 (0.213 g, 1.0 mmol). Yield: 0.73 g (73%). ESI-MS, *m*/*z*: 895.12 $[(M-2H-ClO_4)^+]$, 398.07 $[(M-2H-2ClO_4)^{2+}]$. *Anal.* Calc. for $C_{40}H_{42}Fe_2N_6O_{13}Cl_2$: C, 48.17; H, 4.24; N, 8.43. Found: C, 48.12; H, 4.19; N, 8.39%.

2.3.3. $[Fe_2(O)(OBz)_2(L3)_2](ClO_4)_2$ (**3**)

Complex **3** was prepared using the above general procedure using L3 (0.202 g, 1.0 mmol). Yield: 0.76 g (78%). ESI-MS, *m*/*z*: 872.53 $[(M-2H-ClO_4)^+]$, 751.00 $[(M-2H-BzO-ClO_4)^+]$, 387.00 $[(M-2H-2ClO_4)^{2+}]$. *Anal.* Calc. for $C_{36}H_{40}Fe_2N_8O_{13}Cl_2$: C, 44.33; H, 4.13; N, 11.49. Found: C, 44.39; H, 4.15; N, 11.43%.

2.3.4. $[Fe_2(O)(OBz)_2(L4)_2](ClO_4)_2$ (**4**)

Complex **4** was prepared using the above general procedure using L4 (0.238 g, 1.0 mmol). Yield: 0.65 g (62%). ESI-MS, *m*/*z*: 945.07 $[(M-2H-ClO_4)^+]$, 423.07 $[(M-2H-2ClO_4)^{2+}]$. *Anal.* Calc. for $C_{42}H_{40}Fe_2N_8O_{13}Cl_2$: C, 48.16; H, 3.85; N, 10.70. Found: C, 48.19; H, 3.81; N, 10.74%.

2.3.5. $[Fe_2(O)(OBz)_2(L5)_2](ClO_4)_2$ (**5**)

Complex **5** was prepared as reported [51] earlier. This complex was already well characterized structurally and it possesses a distorted bioctahedral geometry in which each iron atom is coordinated to the oxygen atom of the μ-oxo bridge, two oxygen atoms

of μ-carboxylate bridges and three nitrogen atoms of the 3N ligand, capping the diiron(III) cluster. Yield: 0.74 g (80%). ESI-MS, *m/z*: 827.07 [(M−2H−ClO_4)$^+$], 364.07 [(M−2H−2ClO_4)$^{2+}$]. *Anal.* Calc. for $C_{34}H_{46}Fe_2N_6O_{13}Cl_2$: C, 43.94; H, 4.99; N, 9.04. Found: C, 43.89; H, 5.03; N, 9.09%.

2.3.6. $[Fe_2(O)(OBz)_2(L6)_2](ClO_4)_2$ (**6**)

Complex **6** was prepared as reported [52] earlier. This was already well characterized by X-ray crystallographically and it possesses a distorted bioctahedral geometry in which each iron atom is coordinated to the oxygen atom of the μ-oxo bridge, two oxygen atoms of μ-carboxylate bridges and three nitrogen atoms of the 3N ligand, capping the diiron(III) cluster. Yield: 0.79 g (70%). ESI-MS, *m/z*: 401.38 [(M−2H−BzO)$^{2+}$], 462.45 [(M−2H−2ClO_4)$^{2+}$]. *Anal.* Calc. for $C_{46}H_{42}Fe_2N_{10}O_{13}Cl_2$: C, 49.09; H, 3.76; N, 12.45. Found: C, 49.12; H, 3.72; N, 12.49%.

Caution! The perchlorate salts of the compounds are potentially explosive! Only small quantities of these compounds should be prepared and suitable precautions should be taken when they are handled.

2.4. Catalytic oxidations

In a typical reaction, the oxidant *m*-CPBA (0.8 mol dm^{-3}) was added to a mixture of the diiron(III) complex (1×10^{-3} mmol dm^{-3}) and the alkanes (3 mol dm^{-3}) in a CH_2Cl_2:CH_3CN mixture (4:1 v/v). After 30 min the reaction mixture was quenched with triphenylphosphine, the reaction mixture was filtered over a silica column and then eluted with diethylether. An internal standard (bromobenzene) was added at this point and the solution was subjected to GC analysis. The mixture of organic products was identified by GC-MS and quantitatively analyzed by HP 6890 series GC equipped with an HP-5 capillary column (30 m × 0.32 mm × 2.5 μm) using a calibration curve obtained with authentic compounds. All of the products were quantified using GC (FID) with the following temperature program: injector temperature 130 °C; initial temperature 60 °C, heating rate 10 °C min^{-1} to 130 °C, increasing the temperature to 160 °C at a rate of 2 °C min^{-1}, and then increasing the temperature to 260 °C at a rate of 5 °C min^{-1}; FID temperature 280 °C. GC-MS analysis was performed under conditions identical to those used for GC analysis. The averages of three measurements are reported.

2.5. Physical measurements

Elemental analyses were performed on a Perkin Elmer Series II CHNS/O Analyzer 2400. ^{1}H NMR spectra were recorded on a Bruker 400 MHz NMR spectrometer. Electronic spectra were recorded on an Agilent 8453 Diode Array spectrophotometer. Low temperature spectra were obtained on an Agilent 8453 Diode Array spectrophotometer equipped with an UNISOKU USP-203 cryostat. Electrospray-ionization mass-spectrum (ESI-MS) analyses were recorded on a Micromass Quattro II triple quadrupole mass spectrometer. Cyclic voltammetry (CV) and differential pulse voltammetry (DPV) were performed at 25.0 ± 0.2 °C using a three-electrode cell configuration. A platinum sphere, a platinum plate and Ag(s)/$AgNO_3$ were used as the working, auxiliary and reference electrodes, respectively. The platinum sphere electrode was sonicated for two minutes in dilute nitric acid, dilute hydrazine hydrate and in double distilled water to remove any impurities. The reference electrode for a non-aqueous solution was Ag(s)/Ag$^+$, which consists of a Ag wire immersed in a solution of $AgNO_3$ (0.01 M) and tetra-N-butylammonium perchlorate (0.1 M) in acetonitrile placed in a tube fitted with a Vycor plug. The instruments utilized included an EG & G PAR 273 Potentiostat/Galvanostat and P-IV computer along with EG & G M270 software to carry out the experiments and to acquire the data. The temperature of the electrochemical cell was maintained by a cryo-circulator (HAAKE D8-G). The $E_{1/2}$ value observed under identical conditions for the Fc/Fc$^+$ couple in acetonitrile was 0.102 V with respect to the Ag/Ag$^+$ reference electrode. The experimental solutions were deoxygenated by bubbling research grade nitrogen and an atmosphere of nitrogen was maintained over the solution during measurements. The products were analyzed using a Hewlett Packard (HP) 6890 GC series Gas Chromatograph equipped with a FID detector and a HP-5 capillary column (30 m × 0.32 mm × 2.5 μm). GC-MS analysis was performed on an Agilent GC-MS equipped with 7890A GC series (HP-5 capillary column) and 5975C inert MSD under conditions that were identical to those used for GC analysis.

3. Results and discussion

3.1. Synthesis and characterization of the 3N ligands and diiron(III) complexes

The tridentate 3N ligands L1–L5 were synthesized according to known procedures [53–58], which involve Schiff base condensation of the amines with the corresponding carboxaldehyde followed by reduction with $NaBH_4$. They were characterized by ^{1}H NMR and mass spectrometry. The ligand L6 was prepared by a method involving a Philips condensation [59]. The diiron(III) complexes **1**–**6** were prepared by adding one equivalent of the 3N ligand to an aqueous methanol solution containing a mixture of one equivalent each of $Fe(ClO_4)_3{\cdot}6H_2O$, benzoic acid and triethylamine. All of the complexes are formulated as $[Fe_2(O)(OBz)_2(L)_2](ClO_4)_2$ on the basis of elemental analysis, UV-Vis spectroscopy, ESI-MS and X-ray crystal structures of **5** and **6**. Attempts to grow single crystals of complexes **1**–**4** suitable for X-ray diffraction analysis were unsuccessful. The pyridyl, imidazolyl and sterically hindering 6-methylpyridyl/benzimidazolyl and weakly binding –NMe_2 groups [pK_a (BH^+): pyridine, 5.2; imidazole, 7.01; benzimidazole, 5.4] in the ligands are expected to influence the coordination as well as the electronic properties and reactivities of the diiron(III) complexes. All the complexes, with different linear 3N donor ligands and benzoic acid as a bridging ligand, are expected to mimic the active site environment of the substrate-bound enzyme sMMO and so they have been chosen to model the alkane hydroxylation reactions of the enzyme. The ligands with different nitrogen donors and the benzoate bridging ligand are expected to play an important role in determining the reactivity.

3.2. Electronic spectral studies

In acetonitrile solution all the diiron(III) complexes show two electronic spectral bands located in the range 450–520 nm (ε_{max}, 930–1450 M^{-1} cm^{-1}, Table 1, Fig. 2), which are characteristic [39,50,51,60,61] of O^{2-} → iron(III) LMCT bands in oxo-bridged diiron(III) complexes containing two carboxylate bridges. Four weak spin-forbidden d–d transitions are expected for high-spin octahedral iron(III) complexes; however, only one band around 700 nm is readily observed for all the complexes and the remaining bands are obscured by the more intense LMCT bands. The molar absorptivity of the band around 700 nm is much higher than that observed for mononuclear high-spin octahedral iron(III) complexes [62–69] due to lower symmetry of the dimeric complex with the oxo-bridge and also the spin–spin interaction between the iron(III) centers [62–69]. The oxo-bridge of the complexes remains intact in dichloromethane/acetonitrile solvent mixture as revealed by ESI-MS analysis.

3.3. Electrochemical studies

The electrochemical properties of the diiron(III) complexes **1**–**6** were investigated in an acetonitrile/dichloromethane solvent

Table 1
UV–Vis spectral data and electrochemical data of the diiron(III) complexes in DCM:ACN mixture at 25.0 °C.

Complex	λ_{max} (nm) (ε/M^{-1} cm^{-1})	$E_{p,c}$ (CV) (V)	$E_{1/2}$ (DPV) (V)	Redox process
$[Fe_2(O)(OBz)_2(L1)_2]^{2+}$	454 (1230) 499 (925) 698 (136)	−0.781	−0.685	$Fe^{III}Fe^{III} \rightarrow Fe^{II}Fe^{III}$
$[Fe_2(O)(OBz)_2(L2)_2]^{2+}$	459 (1410) 503(1148) 692 (233)	−0.795	−0.729	$Fe^{III}Fe^{III} \rightarrow Fe^{II}Fe^{III}$
$[Fe_2(O)(OBz)_2(L3)_2]^{2+}$	449 (1450) 498 (1110) 662 (175)	−0.877	−0.805	$Fe^{III}Fe^{III} \rightarrow Fe^{II}Fe^{III}$
$[Fe_2(O)(OBz)_2(L4)_2]^{2+}$	458 (1094) 498 (938) 672 (148)	−0.807	−0.743	$Fe^{III}Fe^{III} \rightarrow Fe^{II}Fe^{III}$
$[Fe_2(O)(OBz)_2(L5)_2]^{2+}$ [51]	466 (1445) 507 (1108) 720 (171)	−0.743	−0.679	$Fe^{III}Fe^{III} \rightarrow Fe^{II}Fe^{III}$
$[Fe_2(O)(OBz)_2(L6)_2]^{2+}$	489 (49) 520 (20) 623 (17)	−0.855	−0.775	$Fe^{III}Fe^{III} \rightarrow Fe^{II}Fe^{III}$

Potential measured *vs.* $Ag/AgNO_3$ (0.001 M, 0.1 M TBAP); add 0.544 V to convert to NHE.

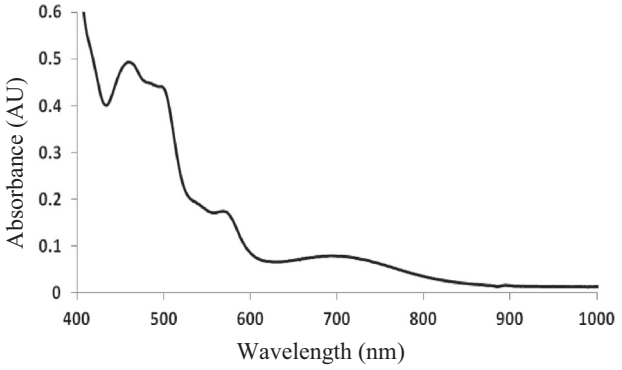

Fig. 2. Electronic spectrum of 4×10^{-4} M $[Fe_2(O)(OBz)_2(L1)_2]^{2+}$ (**1**) in a DCM/acetonitrile mixture at 25 °C.

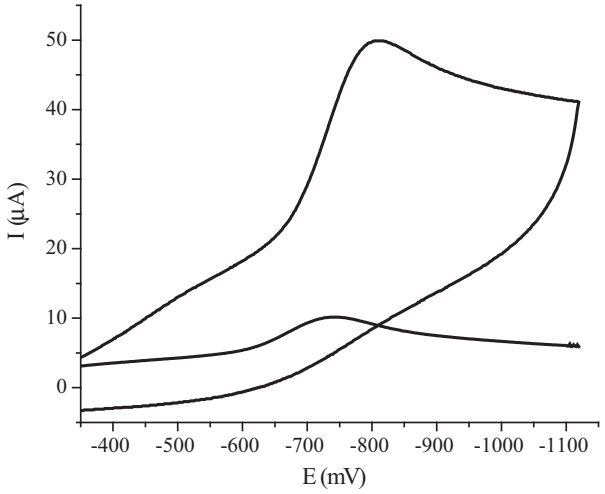

Fig. 3. Cyclic voltammogram (CV)/differential pulse voltammogram (DPV) of 1 mM complex **4** in a DCM/acetonitrile mixture at 25 °C. Supporting electrolyte: 0.1 M TBAP. scan rate: 50 mV s^{-1} for CV and 5 mV/s^{-1} for DPV.

mixture by employing cyclic (CV) and differential pulse voltammetry (DPV) on a stationary platinum electrode. All the complexes show a cathodic peak in the range −0.743 to −0.877 V in the CV, which corresponds to a one electron reduction of the diiron(III) unit, and no coupled oxidation wave is discernible (Fig. 3). The $E_{1/2}$ values of the Fe^{III}/Fe^{II} redox couple (−0.679 to −0.805 V, Table 1) fall in the range observed for a similar type of triply-bridged diiron(III) complexes [50,51,60,70]. The complexes are highly negative, mainly due to the strong coordination of the bridging carboxylate and oxo groups, and follow the trend **5 < 1 < 2 < 4 < 3**; **1 < 6**, revealing the importance of the capping 3N ligands in stabilizing the iron(III) oxidation state in the above complexes with the same benzoate bridges.

$$Fe(III) - O - Fe(III) + e^- \rightarrow Fe(III) - O - Fe(III)$$

Upon replacing one of the pyridylmethyl arms in **1** by a 6-methylpyridyl arm to get **2**, the Fe(III)/Fe(II) redox potential is shifted from −0.685 V (**1**) to a more negative value of −0.729 V (**2**). The 6-methylpyridyl arm, with a sterically hindered nitrogen donor, is expected to coordinate weakly to iron(III) resulting in an increase in the positive charge on iron(III), which is compensated by the stronger coordination of other pyridyl nitrogen donors of the 3N ligand leading to render the reduction of iron(III) more difficult, and hence the more negative redox potential of **2**. Upon replacing one of the pyridylmethyl arms of L1 in **1** by an imidazolylmethyl arm to get **3**, the Fe(III)/Fe(II) redox potential is shifted from −0.685 V (**1**) to a more negative value of −0.805 V (**3**); this reveals that the stronger coordination of the imidazolyl nitrogen [(pK_a (BH^+): pyridine, 5.2; imidazole, 7.01] to the diiron(III) center leads to a decrease in the Lewis acidity of the iron(III) center and hence the more negative value of the redox potential. Similarly, upon changing one of the pyridylmethyl arms of L1 in **1** to a benzimidazolyl methyl arm to get **4**, the $Fe^{III}Fe^{III}/Fe^{III}Fe^{II}$ redox potential of **1** moves towards a more negative value of −0.743 V; this is due to the stronger coordination of the benzimidazolyl nitrogen [(pK_a (BH^+): pyridine, 5.2; benzimidazole, 5.4)]. Also, upon replacing both the pyridylmethyl arms of L1 in **1**, by two strongly σ-bonding benzimidazolyl methyl arms to get **6**, [(pK_a (BH^+): pyridine, 5.2; benzimidazole, 5.4)] a similar decrease in redox potential (−0.743 V) is observed. The replacement of one of the pyridylmethyl arms of L1 in **1** by the $-NMe_2$ group to get **5**, the redox potential is shifted to a less negative value of −0.679 V, revealing that the weaker coordination of the sterically hindering $-NMe_2$ group leads to an increase in the Lewis acidity of the iron(III) centers and hence the higher $Fe^{III}Fe^{III}/Fe^{III}Fe^{II}$ redox potential of the diiron(III) center. Thus the above order of increasing $Fe^{III}Fe^{III}/Fe^{III}Fe^{II}$ redox potentials represents the increasing order of Lewis acidity of the diiron(III) center and also the stability

of the diiron(III) core towards reduction. This is relevant to the reduction of the diiron(III) core in the oxidized form of the sMMO enzyme to obtain the reduced form, which is the active form of the enzyme.

3.4. Functionalization of alkanes

The experimental conditions and results of the catalytic oxidation of alkanes for the diiron(III) complexes **1**–**6** are summarized in Tables 2–4. The conversion of alkanes into hydroxylated products was quantified based on gas chromatographic analysis by using authentic samples and an internal standard (bromobenzene). The catalytic ability of the diiron(III) complexes towards the oxidation of alkanes like cyclohexane, adamantane and cumene was investigated using *m*-CPBA as the oxidant in a dichloromethane/acetonitrile solvent mixture (4:1 v/v) at room temperature. Control reactions performed in the absence of the diiron(III) complexes with *m*-CPBA as the oxidant yielded only very small amounts of the oxidized products (cyclohexane, 3 TON; adamantane, 5 TON; cumene 4 TON), revealing that all the diiron(III) complexes act as catalysts towards the oxidation of alkanes to alcohols. In the presence of the diiron(III) complexes the oxidation of cyclohexane proceeds to give cyclohexanol (A) as the major product, along with cyclohexanone (K) and ε-caprolactone as the minor products. The latter is the over-oxidized product of cyclohexanone in the presence of excess or unreacted *m*-CPBA. All the complexes display efficient alkane hydroxylation with turnover numbers (TON) of 293–401, with good selectivity for the hydroxylation of cyclohexane (A/K, 9.3–12.8; Table 2). The catalytic activity of the diiron(III) complexes towards hydroxylation of cyclohexane follows the trend **5** (Total TON, 411; A/K, 10.1) > **1** (388; 12.8) > **2** (376; 11.5) > **3** (362; 10.3) > **4** (319; 9.3); **1** > **6** (293; 9.5), illustrating the importance of the 3N capping ligands. Very interestingly, the same order of TON is also observed for adamantane oxidation: **5** (Total TON, 437; 3°/2°, 15.7) > **1** (415; 28.1) > **2** (402; 22.1) > **3** (390; 21.3) > **4** (362; 17.8); **1** > **6** (336; 18.9) (Table 3), revealing the involvement of a mechanism the same as that for the cyclohexane oxidation. Thus, all the present diiron(III) complexes show high selectivity in the hydroxylation of cyclohexane (A/K, 9.3–12.8) and adamantane (3°/2°, 15.7–28.1) as well, signifying the involvement of metal-based oxidants rather than non-selective freely diffusing radical species in the alkane hydroxylation [43,37,71,72]. Also, under a nitrogen atmosphere, almost the same type of reactivity pattern is observed supporting the involvement of metal-based oxidants rather than cyclohexylperoxide species in the catalytic reaction.

When the oxidant H_2O_2 or *t*-BuOOH is added to the diiron(III) complexes dissolved in a dichloromethane/acetonitrile solvent mixture at room temperature no spectral change is observed, even after adding triethylamine. Also, the addition of the strong oxidant *m*-CPBA to an acetonitrile solution of the diiron(III) complexes at room temperature produces no significant spectral changes. However, the addition of one equivalent of triethylamine to a reaction mixture containing *m*-CPBA leads to the appearance of a new band in the region of 620–720 nm (Fig. 4), which is ascribed to the adduct species $[Fe_2O(L)_2(BzO)(OOCOC_6H_4Cl)]^{2+}$, formed by replacing one of the bridging carboxylates by *m*-CPBA. During the decay of this adduct in the absence of a substrate no new band characteristic of high-valent intermediate species is observed. Similar observations have been made for the analogous diiron(III) complexes $[Fe_2O(^{i}Bubpa/Bzbpa)_2(OBz)_2]^{2+}$ and $[Fe_2O(L)_2(RCOO)_2]^{2+}$ upon addition of *m*-CPBA followed by triethylamine. We have already characterized the adduct species [50,51] formed as $[Fe_2O(^{i}Bubpa/Bzbpa)_2(OBz)(OOCOC_6H_4Cl)]^{2+}$ and $[Fe_2O(L)_2(RCO_2)(OOCOC_6H_4Cl)]^{2+}$ by using UV-Vis spectroscopy and ESI-MS techniques. Also for these adducts was no intermediate discerned during their decay in the absence of a substrate. Such an intermediate species has been proposed to be formed initially in alkane hydroxylation reactions catalyzed by the complexes $[Fe_2(O)(OBz)_2(^{i}Bubpa/Bzbpa)_2](ClO_4)_2$ [50,51] and $[Fe_2(O)(OAc)_2(hexpy)](ClO_4)_2$ [39] using *m*-CPBA as oxidant. So, we now propose that the acyloxo adduct species $[Fe_2O(L)_2(BzO)(OOCOC_6H_4Cl)]^{2+}$ (Scheme 3) undergoes either O–O bond homolysis or O-O bond heterolysis leading to the formation respectively of high-valent Fe^{IV}=O or Fe^{V}=O intermediate species, which are involved in the selective hydroxylation of alkanes. We have already proposed [50,51] a similar mechanistic pathway to successfully illustrate the selective hydroxylation of cyclohexane by $[Fe_2O(^{i}Bubpa/Bzbpa)_2(OBz)_2]^{2+}$ and $[Fe_2O(L)_2(RCO_2)(OOCOC_6H_4Cl)]^{2+}$.

This is similar to the reaction of a mononuclear iron(III) species with *m*-CPBA to give a benzoylperoxoiron(III) species, which undergoes O–O bond heterolysis to afford an Fe^{V}=O intermediate and *m*-chlorobenzoic acid as a byproduct, and/or O–O bond homolysis to yield an Fe^{IV}=O intermediate and chlorobenzene as a byproduct. It is expected that the distinct nature of the ligand donor atom would determine which one of the two mechanistic pathways operates predominantly. Also, very recently, Que et al. have reported that the complex cation $[Fe^{II}(N4Py)(CH_3CN)]^{2+}$, where N4Py is *N*,*N*-bis(2-pyridylmethyl)-*N*-(bis-2-pyridylmethyl)amine, promotes O–O bond heterolysis, while the cation $[Fe^{III}(N4Py)(CH_3CN)]^{3+}$ favors O–O bond homolysis, and they concluded that the nature of the O–O bond cleavage is dependent on the oxidation state of iron [72]. Also, high-valent Fe^{IV}=O species have been invoked as the key intermediates in C–H bond functionalization by enzymes, as well as their model complexes [7–11,73]. Further, the involvement of a high-valent Fe^{V}=O species has been proposed [74] in the hydroxylation of alkanes using hydrogen peroxide in the presence of the iron(II) complex $[Fe(^{Me2}PyTACN)(OTf)_2]$, where ^{Me2}PyTACN is *N*,*N*-dimethyl-*N*'-(pyrid-2-ylmethyl)triazacyclononane, as a catalyst. For the present complexes, we have observed the formation of chlorobenzene up to 60% based on the total TON, which reveals that up to 60% of the oxidized products are formed due to the involvement of high-valent Fe^{IV}=O species. This observation supports the proposed formation of the adduct species $[Fe_2O(L)_2(BzO)(OOCOC_6H_4Cl)]^{2+}$, which undergoes O–O bond homolysis leading to generate the Fe^{IV}=O species involved in the catalytic reaction, and chlorobenzene is formed by the decarboxylation of the chlorobenzoate radical. As chlorobenzene is produced only up to 60% compared with the total TON, it is clear that some other intermediate species is also involved in the hydroxylation reaction to produce the remaining hydroxylated products. Also, the formation of 3-chlorobenzoic acid supports the formation of high-valent Fe^{V}=O species in the selective hydroxylation of alkanes through heterolysis of

Table 2
Products of oxidation of cyclohexane catalyzed[a] by the diiron(III) complexes.

Complex	Cyclohexane (TON)			Total TON[c]	A/K[d]	Yield[e] (%)
	-ol[b]	-one[b]	ε-caprolactone			
1	360	20	08	388	12.8	48.5
2	346	20	10	376	11.5	47.0
3	330	18	14	362	10.3	45.3
4	280	16	14	310	9.3	38.8
5 [51]	374	23	14	411	10.1	51.3
6	265	16	12	293	9.5	36.6

[a] Reaction conditions: Catalyst (1×10^{-3} mmol dm^{-3}), Substrate (3 mol dm^{-3}), Oxidant (0.8 mol dm^{-3}) in DCM:ACN solvent mixture (9:1 v/v).
[b] -ol = cyclohexanol and -one = cyclohexanone.
[c] Total TON = no. of mmol of product/no. of mmol of catalyst.
[d] A/K = TON of -ol/(TON of -one + TON of ε-caprolactone).
[e] Yield based on the oxidant.

Table 3
Products of oxidation of adamantane catalyzed[a] by the diiron(III) complexes.

Complex	Adamantane (TON)			Total TON[c]	Selectivity[d]	Yield[e] (%)
	1-adol[b]	2-adol[b]	2-adone[b]		3°/2°	
1	375	40	–	415	28.1	69.1
2	354	48	–	402	22.1	67.0
3	342	38	10	390	21.3	65.0
4	310	44	08	362	17.8	60.3
5 [51]	367	58	12	437	15.7	72.8
6	290	35	11	336	18.9	56.0

[a] Reaction conditions: Catalyst (1×10^{-3} mmol dm^{-3}), Substrate (1 mol dm^{-3}), Oxidant (0.6 mol dm^{-3}) in DCM:ACN solvent mixture (4:1 v/v).
[b] 1-adol = 1-adamantanol, 2-adol = 2-adamantanol and 2-adone = 2-adamantanone.
[c] TON = no. of mmol of product/no. of mmol of catalyst.
[d] 3°/2° = (TON of 1-adol × 3)/(TON of 2-adol + TON of 2-adone).
[e] Yield based on the oxidant.

Table 4
Products of oxidation of cumene catalyzed[a] by the diiron(III) complexes.

Complex	2-Phenyl-2-propanol	Total TON[b]	Yield[c] (%)
1	171	171	21.4
2	136	136	17.0
3	138	138	17.3
4	110	110	13.8
5	162	162	20.3
6	102	102	12.8

[a] Reaction conditions: Catalyst (1×10^{-3} mmol dm^{-3}), Substrate (3 mol dm^{-3}), Oxidant (0.8 mol dm^{-3}) in DCM:ACN solvent mixture (9:1 v/v).
[b] Total TON = no. of mmol of product/no. of mmol of catalyst.
[c] Yield based on the oxidant.

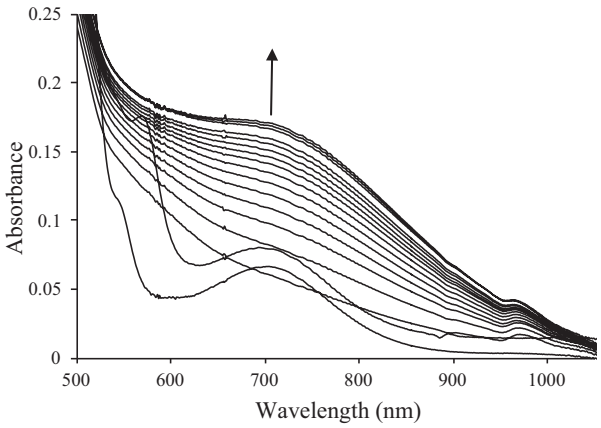

Fig. 4. Reaction of complex **1** with *m*-CPBA (5 equiv.) and triethylamine (1 equiv.) followed by UV–Vis spectroscopy at room temperature.

the O–O bond in the acyloxo adduct species. A similar but mononuclear intermediate Fe^{V}=O species $[Fe(TAML)(O)]^{-}$, derived from the reaction of the iron(III) precursor with *m*-CPBA in butrylonitrile solution at −60 °C, has been already characterized [75] and the stability of the intermediate species is traced to the strong σ-coordination of the tetra-anionic macrocyclic tetra-amide ligand TAML.

For complex **1** the spectral bands characteristic of triply-bridged diiron(III) complexes disappear after approximately 50 turnovers, revealing that the diiron(III) core degrades slowly during catalysis. This suggests that after approximately 50 turnovers a new active metal-based mononuclear intermediate species, $[Fe(L)(PhCO_2)(Sol)_2]^{2+}$, is formed, which is responsible for the highly selective hydroxylation of alkanes to alcohols. We have observed earlier [50] the breaking of the dimeric core of $[Fe_2O(^{i}Bubpa/Bzbpa)_2(OBz)_2]^{2+}$ after approximately 50 turnovers. Kodera et al. observed [39] only a total of 280 turnovers for the hydroxylation of cyclohexane using the diiron(III) complex $[Fe_2O(hexpy)(OAc)](ClO_4)_2$, with the dinucleating ligand as a catalyst and *m*-CPBA as the oxidant. So our observation of a high total TON and better A/K ratio for the present complexes reveal that the mononuclear $[Fe(L)(BzO)(Sol)_2]^{2+}$ species formed by breaking the dimeric core also act as catalysts.

3.5. Cyclohexane oxidation

The ability of the complexes to catalyze the oxidation of cyclohexane varies in the order **5** > **1** > **2** > **3** > **4**; **1** > **6**, as mentioned above. Complex **1** catalyses the oxidation of cyclohexane to give a total TON of 388 (cyclohexanol, 360 TON; cyclohexanone, 20 TON; ε-caprolactone, 8 TON) with good alcohol selectivity (A/K, 12.8). Upon replacing one of the pyridylmethyl arms of L1 in **1** by an imidazolylmethyl arm to get **3**, the oxidation of cyclohexane takes place with a decrease in the total TON from 388 to 362 (cyclohexanol, 330 TON; cyclohexanone, 18 TON; ε-caprolactone, 14 TON) and the selectivity of the alcohol product (A/K, 10.3) as well; also, the decreased Lewis acidity of the metal center due to the stronger coordination of the imidazolyl nitrogen [pK_a (BH^+): pyridine, 5.2; imidazole, 7.01] does not facilitate ligand exchange with the *m*-CPBA anion to form the adduct and the proposed reactive intermediate (cf. above). Similarly, upon replacing one of the pyridylmethyl arms of L1 in **1** by the strongly coordinating benzimidazolylmethyl arm [pK_a (BH^+): pyridine, 5.2; benzimidazole, 5.4] to get **4**, the total TON (310; cyclohexanol, 280 TON; cyclohexanone, 16 TON; ε-caprolactone, 14 TON) as well as the selectivity (A/K, 9.3) decrease. Also, when both the pyridylmethyl arms of L1 in **1** are replaced by two benzimidazolylmethyl arms to get **6**, the total TON decreases from 388 to 293 (cyclohexanol, 265 TON; cyclohexanone, 16 TON; ε-caprolactone, 12 TON) for cyclohexane oxidation and the selectivity of the alcohol also decreases (A/K; 9.5). The steric bulk of the benzimidazolyl groups may also hinder the binding of *m*-CPBA to the diiron(III) center and decrease the concentration of the reactive intermediate. In contrast, upon replacing one of the pyridylmethyl arms of L1 in **1** by the $-CH_2CH_2NMe_2$ arm to give **5**, the oxidation of cyclohexane takes place with an increase in the total TON from 388 to 411 (cyclohexanol, 374 TON; cyclohexanone, 23 TON; ε-caprolactone, 14 TON), but with a decrease in selectivity of the alcohol product (A/K, 10.1). The higher Lewis acidity of the diiron(III) center (cf. above) in **5** enhances the ligand exchange with *m*-CPBA and the formation of the proposed reactive intermediate and hence the catalytic activity. A similar enhancement in Lewis acidity of the diiron(III) center and hence higher catalytic activity is expected [41,51] upon replacing one of the pyridylmethyl arms of L1 in **1** by the 6-methylpyridylmethyl arm to get **2**; however,

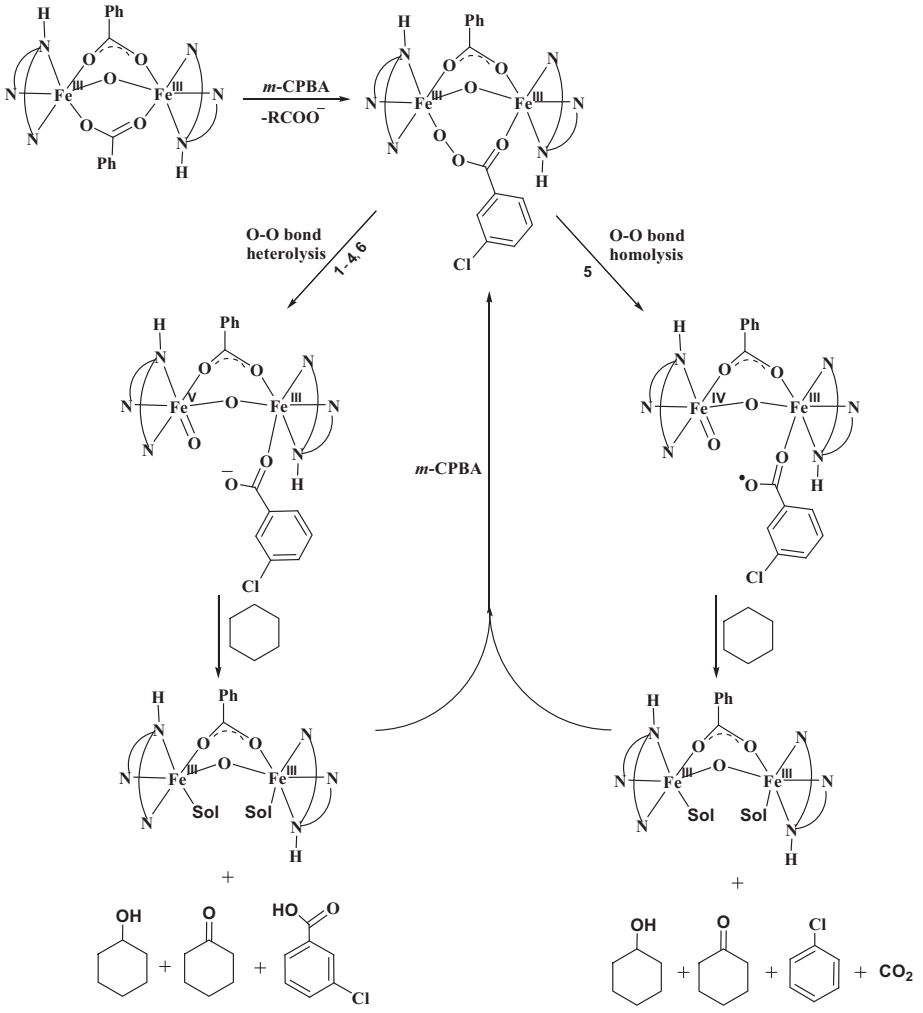

Scheme 3. Proposed mechanism for alkane hydroxylation [51].

the oxidation of cyclohexane takes place with a decrease in both the catalytic activity from 388 TON to 376 (cyclohexanol, 346 TON; cyclohexanone, 20 TON; ε-caprolactone, 10 TON) and the selectivity (A/K, 11.5). So, it is evident that the incorporation of a methyl group, which sterically hinders the coordination of the pyridyl nitrogen, enhances the Lewis acidity of the diiron(III) center, but is compensated by the stronger coordination of the other pyridyl nitrogen leading to an effective decrease in the Lewis acidity of the diiron(III) center, and hence the lower catalytic activity. Thus the Lewis acidity of the diiron(III) center, as modified by the different donor atoms of the capping ligand, dictates the ligand exchange with the oxidant and the formation of the intermediate high-valent oxo species and hence the catalytic activity. Also, a homolytic O–O bond cleavage pathway [72] is suggested to occur predominantly for **5**, with the highest Lewis acidity for the diiron(III) center, while heterolytic O–O bond cleavage is favored for the remaining complexes with lower Lewis acidity.

3.6. Adamantane and cumene oxidation

All the diiron(III) complexes catalyze the oxidation of adamantane efficiently to give 1-adamantanol and 2-adamantanol as the major products, along with 2-adamantanone as a minor product. The ability of the complexes to catalyze the oxidation of adamantane varies in the order **5** (437) > **1** (415) > **2** (402) > **3** (390) > **4** (362); **1** > **6** (336), as for the cyclohexane oxidation, revealing that the same kind of intermediates and ligand stereoelectronic factors are involved in both the oxidation reactions. Complex **1** catalyzes the oxidation of adamantane with a total TON of 415 (1-adamantanol, 375 TON; 2-adamantanol, 40 TON) with a very good selectivity (3°/2°, 28.1), revealing that the reaction involves a metal based oxidant. The catalytic activity of the complex is higher than those previously reported for benzoate-bridged diiron(III) complexes $[Fe_2O(OBz)_2(^{i}Bubpa/Bzbpa)_2](ClO_4)_2$ (Total TON: ^{i}Bubpa, 412; Bzbpa, 329) [50]. The bond selectivity (3°/2°, 28.1) is lower than that for the ^{i}Bubpa (3°/2°, 30.3) complex, but higher than that for the Bzbpa (3°/2°, 26.1) complex [50], suggesting that the capping ligand plays an important role in determining the bond selectivity. Upon introducing the imidazolylmethyl arm into L1 of **1** to get **3**, the oxidation of adamantane takes place with a decrease in both the total TON 390 (1-adamantanol, 342 TON; 2-adamantanol, 38 TON; 2-adamantanone 10 TON) and the 3°/2° (21.3) bond selectivity. As discussed above for the cyclohexane oxidation, the strongly coordinating imidazolyl nitrogen [pK_a (BH^+): pyridine, 5.2; imidazole, 7.01] decreases the ligand exchange of the bridging corboxylate with *m*-CPBA, leading to lower catalytic efficiency (cf. above). A similar decrease in the catalytic activity is observed when one pyridylmethyl arm in L1 of **1** is replaced with one benzimidazolyl arm to get **4**, both the total TON (362; 1-adamantanol, 310 TON; 2-adamantanol, 44 TON; 2-adamantanone 8 TON) and 3°/2° bond selectivity (17.8) decrease. Similarly, on replacement of both the pyridylmethyl arms in **1** by benzimidazolylmethyl arms

to get **6**, the catalytic activity decreases, as illustrated above for the cyclohexane oxidation (Total TON 336; 1-adamantanol, 290 TON; 2-adamantanol, 35 TON; 2-adamantanone 11 TON; bond selectivity 3°/2°, 18.9). Also, the steric bulk of the benzimidazolyl groups may hinder the binding of *m*-CPBA to the diiron(III) center. In contrast, the replacement of the pyridylmethyl arms in L1 of **1** by the bulky $-NMe_2$ group to get **5** increases the total TON to 437 (1-adamantanol, 367 TON; 2-adamantanol, 58 TON; 2-adamantanone 12 TON) and also the bond selectivity (15.7). Interestingly, the catalytic efficiency is higher than those of the previously reported benzoate-bridged complexes (total TON: ^{i}Bubpa, 412; Bzbpa, 329). However, the 3°/2° selectivity for **5** (15.7) is again lower than those of the previously reported [50] complexes (3°/2°: ^{i}Bubpa, 30.3; Bzbpa, 26.1). Similarly, for complex **2** the catalytic oxidation of adamantane takes place with a small decrease in the catalytic activity from 415 TON to 402 with a good selectivity (3°/2°, 22.1), as illustrated above for cyclohexane oxidation (cf. above). Interestingly, complex **2** is very selective in catalyzing adamantane to the alcohol product. All the above observations suggest that the capping ligand plays an important role in determining the selectivity of the alcohol product.

The catalytic activity of the diiron(III) complexes towards the oxidation of cumene has also been investigated and the results are summarized in Table 4. Interestingly, all the complexes catalyze the oxidation of cumene selectively to form 2-phenyl-2-propanol without any side product formation. The oxidation of cumene follows the same order as that for cyclohexane oxidation.

4. Conclusions

We have isolated a few triply-bridged diiron(III) complexes derived from linear 3N ligands and studied their ability to carry out alkane functionalization using *m*-CPBA as an oxidant. All the complexes show spectral and electrochemical properties characteristic of μ-oxo-bridged diiron(III) complexes also containing two carboxylate bridges. The A/K and 3°/2° bond selectivity for hydrocarbon oxidation catalyzed by the present complexes fall in the ranges 9.3–12.8 and 15.7–28.1 respectively. This suggests that the capping ligand plays an important role in determining the selectivity of the product. The observation of high selectivity towards alkane hydroxylation suggests the involvement of an intermediate metal-based oxidant rather than freely diffusing radicals in the oxygenation. The 3°/2° bond selectivity observed for the hydroxylation of adamantane for the diiron(III) complex of the 3N capping ligand with two pyridyl donors (L1) is the highest among the present complexes.

Acknowledgments

We sincerely thank the Council of Scientific and Industrial Research, New Delhi, for a Senior Research Fellowship to M.S. This work was also supported by the Indo-French Centre (IFCPAR) [Scheme No. IFC/A/4109-1/2009/993]. Professor M. Palaniandavar is a recipient of a DST Ramanna Fellowship [Scheme No. SR/S1/RFIC-01/2007 and SR/S1/RFIC-01/2010]. We thank Dr. Balachandran Unni Nair, Central Leather Research Institute, Chennai for providing the ESI-MS facility.

References

[1] D. Riley, M. Stern, J. Ebner, in: D.H.R. Barton, A.E. Martell, D.T. Sawyer (Eds.), The Activation of Dioxygen and Homogeneous Catalytic Oxidation, Plenum, New York, 1993, p. 31.
[2] J. Colby, H. Dalton, R. Whittenbury, Annu. Rev. Microbiol. 33 (1979) 481.
[3] H. Dalton, Adv. Appl. Microbiol. 26 (1980) 71.
[4] J.B. Vincent, G.L. Olivier-Lilley, B.A. Averill, Chem. Rev. 90 (1990) 1447.
[5] J.D. Lipscomb, Annu. Rev. Microbiol. 48 (1994) 317.
[6] A.L. Feig, S.J. Lippard, Chem. Rev. 94 (1994) 759.
[7] B.J. Waller, J.D. Lipscomb, Chem. Rev. 96 (1996) 2625.
[8] M. Baik, M. Newcomb, R.A. Friesner, S.J. Lippard, Chem. Rev. 103 (2003) 2385.
[9] M. Costas, M.P. Mehn, M.P. Jensen, L. Que Jr., Chem. Rev. 104 (2004) 939.
[10] E.Y. Tshuva, S.J. Lippard, Chem. Rev. 104 (2004) 987.
[11] S.V. Kryatov, E.V. Rybak-Akimova, S. Schindler, Chem. Rev. 105 (2005) 2175.
[12] A.C. Rosenzweig, C.A. Frederick, S.J. Lippard, P. Nordlund, Nature 366 (1993) 537.
[13] L. Westerheide, M. Pascaly, B. Krebs, Curr. Opin. Chem. Biol. 4 (2000) 235.
[14] M. Merkx, D.A. Kopp, M.H. Sazinsky, J.L. Blazyk, J. Muller, S.J. Lippard, Angew. Chem., Int. Ed. 40 (2001) 4000.
[15] R.E. Stenkamp, Chem. Rev. 94 (1994) 715.
[16] D.T. Logan, X.D. Su, A. Aberg, K. Regnstrom, J. Hajdu, H. Eklund, P. Nordlund, Structure 4 (1996) 1053.
[17] A. Jordan, P. Reichard, Annu. Rev. Biochem. 67 (1998) 71.
[18] J. Stubbe, Curr. Opin. Chem. Biol. 7 (2003) 183.
[19] P.C. Wilkins, R.C. Wilkins, Coord. Chem. Rev. 79 (1987) 195.
[20] S.J. Lippard, Angew. Chem., Int. Ed. Engl. 27 (1988) 344.
[21] D.M. Kurtz Jr., Chem. Rev. 90 (1990) 585.
[22] J.B. Vincent, G.L. Oliver-Lilley, B.A. Averill, Chem. Rev. 90 (1990) 1447.
[23] E.I. Solomon, F. Tuczek, D.E. Root, C.A. Brown, Chem. Rev. 94 (1994) 827.
[24] W. Nam, R. Ho, J.S. Valentine, J. Am. Chem. Soc. 113 (1991) 7052.
[25] K. Chen, L. Que Jr., Chem. Commun. (1999) 1375.
[26] K. Chen, L. Que Jr., Angew. Chem., Int. Ed. 38 (1999) 2227.
[27] K. Chen, L. Que Jr., J. Am. Chem. Soc. 123 (2001) 6327.
[28] Y. Mekmouche, S. Ménage, C. Toia-Duboc, M. Fontecave, J.-B. Galey, C. Lebrun, J. Pécaut, Angew. Chem., Int. Ed. 40 (2001) 949.
[29] K. Chen, M. Costas, L. Que Jr., J. Chem. Soc., Dalton Trans. (2002) 672.
[30] M. Fontecave, S. Ménage, C. Duboc-Toia, Coord. Chem. Rev. 178 (1998) 1555.
[31] W.H. Armstrong, S.J. Lippard, J. Am. Chem. Soc. 105 (1983) 4837.
[32] K. Wieghardt, K. Pohl, W. Gebert, Angew. Chem., Int. Ed. Engl. 22 (1983) 727.
[33] K. Wieghardt, I. Tolksdorf, W. Herrmann, Inorg. Chem. 24 (1985) 1230.
[34] K.B. Jensen, C.J. McKenzie, O. Simonsen, H. Toftlund, A. Hazell, Inorg. Chim. Acta 257 (1997) 163.
[35] S. Nishino, H. Hosomi, S. Ohba, H. Matsushima, T. Tokii, Y. Nishida, J. Chem. Soc., Dalton Trans. (1999) 1509.
[36] J.B. Vincent, J.C. Huffmann, G. Christou, Q. Li, M.A. Nanny, D.N. Hendrickson, R.H. Fong, R.H. Fish, J. Am. Chem. Soc. 110 (1988) 6898.
[37] R.H. Fish, M.S. Konings, K.J. Oberhausen, R.H. Fong, W.M. Yu, G. Christou, J.B. Vincent, D.K. Coggin, R.M. Buchanan, Inorg. Chem. 30 (1991) 3002.
[38] N. Kitajima, H. Fukui, Y. Moro-oka, J. Chem. Soc., Chem. Commun. (1988) 485.
[39] M. Kodera, H. Shimakoshi, K. Kano, Chem. Commun. (1996) 1737.
[40] M. Kodera, H. Shimakoshi, M. Nishimura, H. Okawa, S. Iijima, K. Kano, Inorg. Chem. 35 (1996) 4967.
[41] M. Kodera, Y. Taniike, M. Itoh, Y. Tanahashi, H. Shimakoshi, K. Kano, S. Hirota, S. Iijima, M. Ohba, H. Okawa, Inorg. Chem. Commun. 40 (2001) 4821.
[42] M. Itoh, M. Kodera, K. Kano, J. Inorg. Biochem. 96 (2003) 158.
[43] R.M. Buchanan, S. Chen, J.F. Richardson, M. Bressan, L. Forti, A. Morvillo, R.H. Fish, Inorg. Chem. 33 (1994) 3208.
[44] D. Tetard, J.-B. Verlhac, J. Mol. Catal. A: Chem. 113 (1996) 223.
[45] R.A. Leising, J. Kim, M.A. Pérez, L. Que Jr., J. Am. Chem. Soc. 115 (1993) 9524.
[46] I.W.C.E. Arends, K.U. Ingold, D.D.M. Wayner, J. Am. Chem. Soc. 117 (1995) 4710.
[47] T. Okuno, S. Itoh, S. Ohba, Y. Nishida, J. Chem. Soc., Dalton Trans. (1997) 3547.
[48] S. Ménage, J.-B. Galey, J. Dumats, G. Hussler, M. Seité, I.G. Luneau, G. Chottard, M. Fontecave, J. Am. Chem. Soc. 120 (1998) 13370.
[49] E. Pardo, F. Lloret, R. Carrasco, M.C. Muñoz, T.T. Sánchez, R.R. García, Inorg. Chim. Acta 357 (2004) 2713 (and references therein).
[50] K. Visvaganesan, E. Suresh, M. Palaniandavar, Dalton Trans. (2009) 3814.
[51] M. Balamurugan, E. Suresh, M. Palaniandavar, Inorg. Chem. (2013) Submitted.
[52] P.G. Romero, N.C. Pastor, A.B. Hussein, G.B. Jameson, J. Am. Chem. Soc. 110 (1988) 1988.
[53] M. Velusamy, R. Mayilmurugan, M. Palaniandavar, J. Inorg. Biochem. 99 (2005) 1032.
[54] N. Anitha, M. Palaniandavar, Dalton Trans. 40 (2011) 1188.
[55] T. Dhanalakshmi, E. Suresh, M. Palaniandavar, Dalton Trans. (2009) 8317.
[56] K. Sundaravel, E. Suresh, M. Palaniandavar, Inorg. Chim. Acta 363 (2010) 2768.
[57] D.C. Crans, A.D. Keramidas, S.S. Amin, O.P. Anderson, S.M. Miller, J. Chem. Soc., Dalton Trans. (1997) 2799.
[58] L.A. Cescon, A.R. Day, J. Org. Chem. 27 (1962) 581.
[59] M.A. Philips, J. Chem. Soc. (1928) 2393.
[60] W.H. Armstrong, A. Spool, G.C. Papaefthymiou, R.B. Frankel, S.J. Lippard, J. Am. Chem. Soc. 106 (1984) 3653.
[61] P. Gomez-Romero, N. Casan-Pastor, A. Ben-Hussein, G.B. Jameson, J. Am. Chem. Soc. 110 (1988) 1988.
[62] R. Viswanathan, M. Palaniandavar, T. Balasubramanian, P.T. Muthiah, Inorg. Chem. 37 (12) (1998) 2943.
[63] M. Velusamy, R. Mayilmurugan, M. Palaniandavar, Inorg. Chem. 43 (2004) 6284.
[64] K. Visvaganesan, R. Mayilmurugan, E. Suresh, M. Palaniandavar, Inorg. Chem. 46 (2007) 10294.
[65] R. Mayilmurugan, E. Suresh, M. Palaniandavar, Inorg. Chem. 46 (2007) 6038.
[66] K. Sundaravel, T. Dhanalakshmi, E. Suresh, M. Palaniandavar, Dalton Trans. (2008) 7012.

[67] R. Mayilmurugan, K. Visvaganesan, E. Suresh, M. Palaniandavar, Inorg. Chem. 48 (2009) 8771.
[68] K. Sundaravel, E. Suresh, K. Saminathan, M. Palaniandavar, Dalton Trans. 40 (2011) 8092.
[69] K. Sundaravel, M. Sankaralingam, E. Suresh, M. Palaniandavar, Dalton Trans. 40 (2011) 8444.
[70] J.-A.R. Hartman, R.L. Rardin, P. Chaudhuri, K. Pohl, K. Wieghardt, B. Nuber, J. Weiss, G.C. Papaefthymiou, R.B. Frankel, S.J. Lippard, J. Am. Chem. Soc. 109 (1987) 7387.
[71] J. Kaizer, E.J. Klinker, N.Y. Oh, J.-U. Rohde, W.J. Song, A. Stubna, J. Kim, E. Münck, W. Nam, L. Que Jr., J. Am. Chem. Soc. 126 (2004) 472.
[72] K. Ray, S.M. Lee, L. Que Jr., Inorg. Chim. Acta 361 (2008) 1066.
[73] X. Shan, L. Que Jr., J. Inorg. Biochem. 100 (2006) 421.
[74] A. Company, L. Gómez, M. Güell, X. Ribas, J.M. Luis, L. Que Jr., M. Costas, J. Am. Chem. Soc. 129 (2007) 15766.
[75] F.T. Oliveira, A. Chanda, D. Banerjee, X. Shan, S. Mondal, L. Que Jr., E.L. Bominaar, E. Münck, T.J. Collins, Science 315 (2007) 835.